

# Preparation and thermomechanical characterisation of aluminum titanate flexible ceramics

C. Babelot · A. Guignard · M. Huger ·  
C. Gault · T. Chotard · T. Ota · N. Adachi

Received: 21 April 2010 / Accepted: 3 September 2010 / Published online: 25 September 2010  
© Springer Science+Business Media, LLC 2010

**Abstract** Flexible ceramics may be useful, for example to process refractory materials with an improved resistance to thermal shocks. A natural flexible sandstone, itacolumite, is mainly constituted of interlocked quartz grains and contains microcracks. Its microstructure allows some free motion between grains that induces its flexibility. The aim of this study is to prepare and characterize flexible aluminum titanate ceramics by mimicking the microstructure of itacolumite. Aluminum titanate (AT) has a high thermal expansion anisotropy that induces grain boundary microcracking leading to flexibility. Here, the flexibility is the capacity of the material to endorse large strain-to-rupture level. This concept is also closely related to a low value of the stiffness induced by damage mechanisms. In this study, the flexibility has been estimated by the measurement of the deflection at fracture on three-point bending test. By preparing AT samples sintered according to different heating cycles, the correlations between the sintering cycle, the microstructure and the flexibility have been studied. Grain size and microcrack width have been observed by scanning electron microscopy. A major parameter for flexibility is the microcrack volume fraction within the sample. Three types of AT materials have been processed:

non flexible (NF), flexible (F), and very flexible (VF). Their thermal and mechanical behaviors have been investigated and showed that NF has a brittle behavior while F and VF have a nonlinear ductile one. This was found to be due to grain boundary microcracks network and to the interlocking of grains. VF is more flexible than F because its microcracks are wider. Flexibility improves the thermal shock resistance: F and VF have a higher thermal shock resistance than NF. Moreover, thermal expansion measurements during thermal cycles showed anomalous effects induced by crack closure when heating and crack opening when cooling.

## Introduction

Ceramics are known to be stiff, high-strength but brittle materials. If this brittleness could be overcome, it should be possible to expand the use of ceramic materials to a lot of current applications which require to withstand high strain levels before rupture. In opposition to classical brittle ceramics these materials are called flexible ceramics. They may be highly useful, for example as anti-vibration materials and as refractory materials to resist to thermal shocks and to failure induced by thermal cycling. If many theoretical and experimental works have been devoted to the study of the thermal shock resistance of brittle ceramic materials [1–4], the case of flexible ceramics, which are generally characterized by the highly non linear stress–strain behavior in tension and by unusual thermal expansion effects at low temperature, are not so much documented in literature. It was previously observed that a natural sandstone, itacolumite, has a specific microstructure which allows it to be flexible [5], as shown by the spectacular deflection in bending of a plate observed in Fig. 1.

---

C. Babelot · A. Guignard · M. Huger · C. Gault ·  
T. Chotard (✉)

Groupe d'Etude des Matériaux Hétérogènes (GEMH),  
ENSCI, Centre Européen de la Céramique,  
12 rue Atlantis, 87068 Limoges, France  
e-mail: thierry.chotard@unilim.fr

M. Huger  
e-mail: marc.huger@unilim.fr

T. Ota · N. Adachi  
Ceramics Research Laboratory,  
Nagoya Institute of Technology, Tajimi, Japan

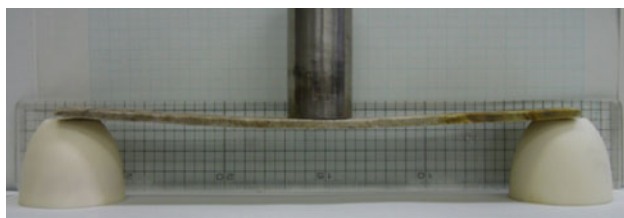


**Fig. 1** Example of flexibility of an itacolumite sample

The reason to achieve such a property is that this material contains numerous intergranular cracks associated to a specific grain shape which make them to be interlocked like a jigsaw puzzle.

In order to assess a similar property, aluminum titanate ( $\text{Al}_2\text{TiO}_5$ ) ceramics (AT) samples were prepared by using a process leading to a microstructure mimicking that of itacolumite. In previous study, other flexible ceramics have been realized by the same way [6]. In an AT polycrystal, the grain boundary microcracking occurring during the cooling process is due to the high thermal expansion anisotropy of its three crystallographic axes:  $\alpha_a = -2.9 \times 10^{-6} \text{ K}^{-1}$ ,  $\alpha_b = 10.3 \times 10^{-6} \text{ K}^{-1}$ , and  $\alpha_c = 20.1 \times 10^{-6} \text{ K}^{-1}$  [7]. In this study three types of AT ceramics have been processed: non flexible (NF), flexible (F), and very flexible (VF). Their thermal and mechanical behaviors are then studied.

## Materials and experimental procedures

### Material synthesis

Granulated industrial powder (TM-20P, Marusu, Japan) was used to elaborate the samples. An XRD phase identification method has revealed that the chosen industrial powder is well stabilized. XRD-pattern of grinded sintered powder is shown in Fig. 2. The peaks are only associated to aluminum titanate, neither to corundum ( $\text{Al}_2\text{O}_3$ ) nor to rutile ( $\text{TiO}_2$ ), which means that there is no decomposition phenomenon.

The size of granulates ranges from 50 to 150  $\mu\text{m}$ , and the size of the grains ranges from 0.1 to 1.5  $\mu\text{m}$ . The samples were shaped by uniaxial pressing at 25 MPa. They were then heated from room temperature to 300  $^\circ\text{C}$  at 1.5  $^\circ\text{C}/\text{min}$ , from 300 to 500  $^\circ\text{C}$  at 0.5  $^\circ\text{C}/\text{min}$ , from 500 to 1100  $^\circ\text{C}$  at 1.5  $^\circ\text{C}/\text{min}$ , from 1100 to 1300  $^\circ\text{C}$  at 2  $^\circ\text{C}/\text{min}$ , and finally from 1300  $^\circ\text{C}$  to the sintering temperature at 1.5  $^\circ\text{C}/\text{min}$ . This slow heating cycle was found to be necessary to optimize debinding. Different sintering temperatures, dwell time, and cooling rate were applied in order to produce different types of microstructure in terms of grain size, microcracking width, and grain boundary aspect. The

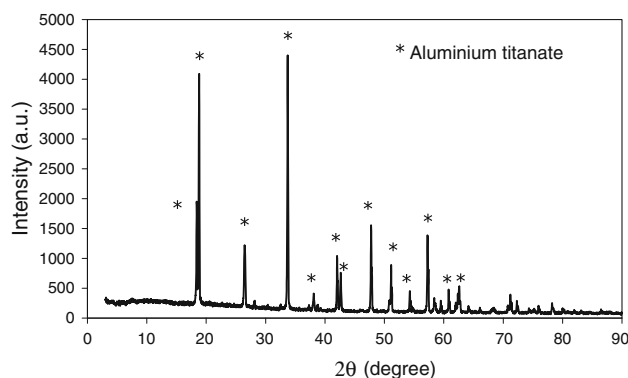


**Fig. 2** XRD-pattern of sintered-AT powder

chosen sintering temperatures are 1500, 1550, or 1600  $^\circ\text{C}$ , dwell times of 1, 4, 8, or 16 h. The cooling time is 4 (fast cooling) or 12 h (slow cooling).

### Mechanical behavior investigation

Mechanical behavior has been studied by three-point bending tests made on parallelepipedic samples ( $100 \times 12.6 \times 11 \text{ mm}^3$ ) on a substantial amount of samples (between four and six samples) to assess the reliability of measurements, using a AGS-J Shimadzu (10 kN) device with a constant crosshead displacement velocity of 1  $\text{mm min}^{-1}$ . The determined parameters are the modulus of rupture (MOR), which corresponds to the maximum stress reached on the stress–deflection curves and the central deflection taken at the same point. Thus this value, expressed in millimeter, strongly depends on the sample thickness. Therefore, samples that are compared to each other have the same dimensions. Concerning the presentation of the curves, the deflection–stress coordinates may not be the best suitable ones for plotting the results. Indeed as the behavior of the material is probably very different in tension and in compression, the moving of the neutral plane can probably affect the calculation of stresses. Hence deflexion–load coordinates would appear more suitable to plot the results, but after a calculation based on the mechanic of material it appears that for this kind of behavior, the error between deflection–stress representation and the deflexion–load one is less than 7%. Obviously speaking, that is why this kind of plotting has been adopted.

### Evaluation of microcracking

In order to estimate a microcracking parameter, we assumed that, the microcracked state of a sample could be defined from two basic characteristics: the maximum width of the intergranular microcrack ( $W_m$ ) and the grain boundary microcracking area  $S$  (related to the microcracked surface between grains) (Fig. 3).

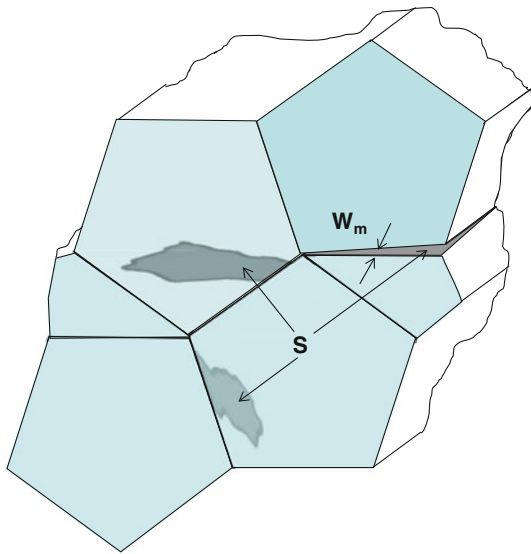


**Fig. 3** Scheme of microstructure and definition of microcracking parameters

A “microcracked volume fraction” can be deduced from these two characteristics after normalisation to the overall volume of the sample. This parameter is evaluating thanks to basic observations and analysis carried out on scanning electron microscopy (SEM) micrographies taken from raw surface of sintered samples.

#### Measurement of Young’s modulus by ultrasonic pulse-echography

Young’s moduli have been measured by ultrasonic pulse-echography at room temperature in infinite mode in samples with two parallel faces. This experiment is carried out by the determination of ultrasonic velocities of both longitudinal and transversal waves [8, 9]. From these measurements, the value of Young’s modulus is calculated through the density of the material  $\rho$ .

#### Thermal expansion measurement

Thermal expansion measurements have been carried out in air using a Setaram vertical dilatometer with a thermal cycle up to 1400 °C. Samples were parallelepipedic with typical dimensions of  $5 \times 5 \times 10 \text{ mm}^3$  and feature smooth and parallel surfaces. The detailed thermal cycle is as follows:

- heating at a rate of  $3 \text{ °C min}^{-1}$  from room temperature to 1400 °C
- no dwell at 1400 °C
- cooling at a rate of  $3 \text{ °C min}^{-1}$  from 1400 °C to room temperature.

#### Thermal shock resistance

Thermal shock process has been applied on aluminum titanate samples. It consists in introducing a sample into a furnace at 1000 °C and then quenching it into water (at room temperature) after a 30-min equilibrium period. A conventional determination of thermal shock resistance has been carried out by comparing the results of the MOR (obtained in three-points bending test) determined before and after the thermal shock sollicitation.

## Results and discussion

### Influence of the sintering thermal cycles on the characteristics of samples

This paragraph presents the results of a multi-parametric study concerning the sintering cycle (sintering temperature, dwell, and cooling time) in terms of mechanical behavior and microstructure of the obtained material.

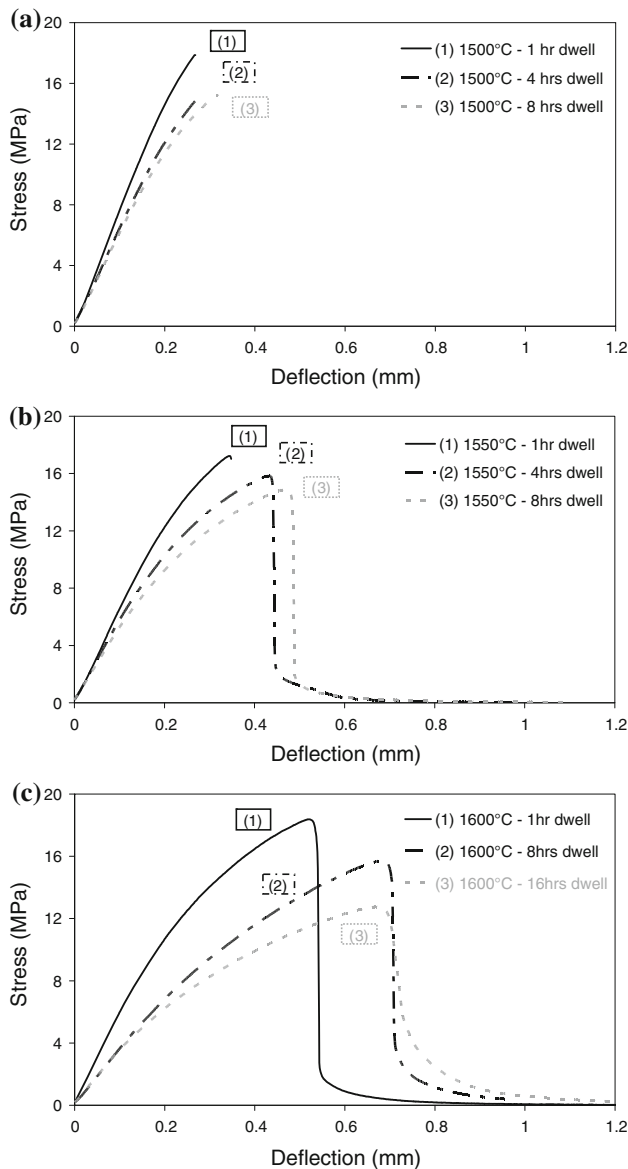
#### Mechanical behavior

Figure 4 shows the effect of dwell time on the mechanical behavior after sintering at different temperatures ( $T_S = 1500, 1550, \text{ and } 1600 \text{ °C}$ ). The cooling time is 4 h (fast cooling).

One observes that the conventional flexibility (deflection at fracture) increases with dwell time up to a limit:

- At  $T_S = 1500 \text{ °C}$ , whatever the sintering time, the samples have a low flexibility: it shows a poorly non linear behavior and a brittle rupture. Moreover, the strength decreases with the sintering dwell.
- At  $T_S = 1550 \text{ °C}$ , it appears that the behavior strongly depends of the sintering dwell. After a dwell time of 1 h, the sample exhibits a low flexibility and a brittle behavior. But after dwell times of 4 h or more, the samples present a flexible behavior with a stress peak. In any case, the strength defined as the peak stress decreases with the dwell time.
- At  $T_S = 1600 \text{ °C}$ , for dwell times of 1, 8, and 16 h the samples have a nonlinear and flexible behavior (existence of a post-peak). Between 1 and 8 h, the flexibility increases and the strength decreases. Between 8 and 16 h, the strength decreases but the flexibility remains the same.

Table 1 summarizes the effects of the sintering temperature ( $T_S = 1500, 1550, \text{ and } 1600 \text{ °C}$ ) and of the dwell time (1, 4, 8, and 16 h) on the conventional flexibility (defined as the deflection at rupture). The cooling time was 4 h (fast cooling).



**Fig. 4** Effect of dwell time on mechanical behavior of AT samples sintered at different temperatures: **a** 1500 °C, **b** 1550 °C, and **c** 1600 °C

**Table 1** Conventional flexibility (mm) versus temperature and dwell time of sintering (cooling time 4 h)

Dwell time (h)	Sintering temperature (°C)		
	1500	1550	1600
1	0.22	0.32	0.5
4	0.22	0.43	–
8	0.26	0.48	0.7
16	–	–	0.7

These observations clearly show that flexibility increases with the sintering temperature, but a maximum is reached after 8 h at 1600 °C.

### Relation with grain growth phenomenon

In the case of AT, intergranular microcracking, which is dependent on grain size is caused by the high thermal expansion anisotropy of crystals. Therefore it is expected to be related to grain growth phenomenon which is dependent on sintering conditions. Table 2 shows the grain size of AT samples sintered in different conditions determined from SEM observations. As classically observed in ceramics, the grain size increases with sintering temperature and dwell time.

The comparison with results given in Table 1 qualitatively confirms that higher the grain size are, higher the flexibility is.

For illustrations, Figs. 5, 6, and 7 report SEM micrographies of the three samples sintered with different conditions. They additionally show that, when the sintering temperature is above 1500 °C, AT samples have needle-type grains, probably related to abnormal grain growth. This phenomenon increases with sintering temperature and dwell time. Needle-type grains induce interlocking between the grains, and this specific microstructure helps to flexibility.

The correlation between the grain morphology (mean size and shape) and the volume fraction of intergranular microcracks after cooling is not easy to establish because it needs to consider two mechanisms.

1-Microcrack initiation which occurs when the intergranular stress due to the differential thermal contraction reaches a critical level when cooling. For given grain size and shape, this initiation occurs at a given temperature  $T_c$ . The relation between grain size and  $\Delta T = T_c - T_s$  has been studied in a previous work [10]. According to the authors, the bigger the grains are, the smaller  $\Delta T$  is. It means that for a given sintering temperature, if the grain size is higher, the microcracking at grain boundary, occurring during the cooling stage, begins at a higher temperature. This explains the effect of dwell time on mechanical behavior results shown before: at a given temperature, flexibility (due to microcracking) increases with dwell time (inducing higher grain growth). Nevertheless at a certain point (16 h dwell at 1600 °C), the grains have grown too much, so that the microcracks network is less dense. It does not improve flexibility.

2-Microcrack opening that is controlled by grain-to-grain sliding mechanisms during cooling, after decohesion. It is

**Table 2** Grain size of sintered AT samples according to sintering temperature and dwell time (cooling rate 4 h)

Sintering temperature (°C)	1500	1550	1550	1600	1600	1600
Dwell time (h)	1	1	8	8	8	16
Grain size (μm)	<20	<30	<40	<50	<150	<200



**Fig. 5** SEM images of sample sintered at 1500 °C, 1 and 4 h dwell and cooling time, respectively; **a**  $\times 500$  magnification, **b**  $\times 2000$  magnification

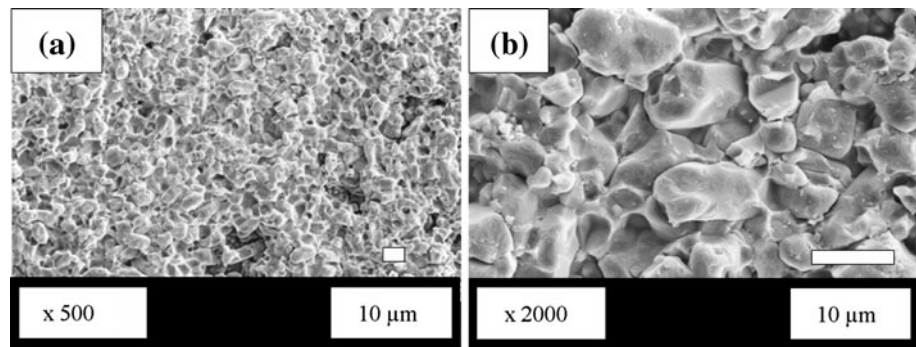


**Fig. 6** SEM images of sample sintered at 1550 °C, 8 and 4 h dwell and cooling time, respectively; **a**  $\times 500$  magnification, **b**  $\times 2000$  magnification

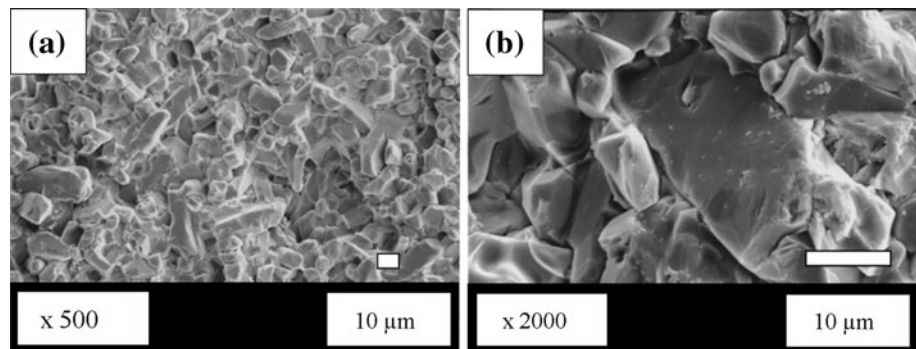
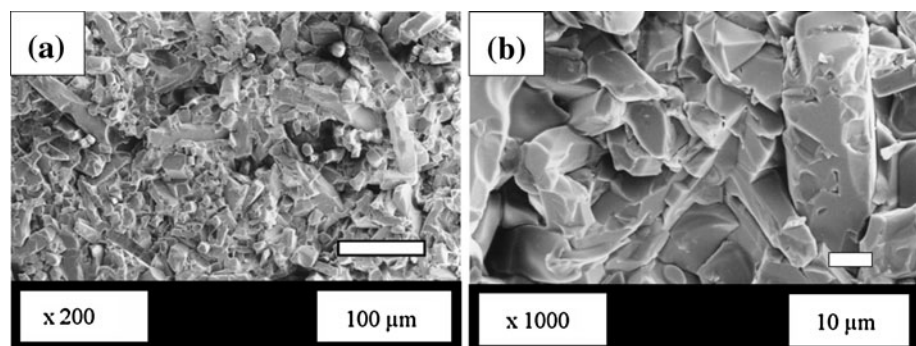


**Fig. 7** SEM images of sample sintered at 1600 °C, 8 and 4 h dwell and cooling time, respectively; **a**  $\times 200$  magnification, **b**  $\times 1000$  magnification



probable that this effect is favored by a high value of  $T_c$  and a low cooling rate, which allows the relaxation of sliding stresses during a longer time. Therefore the variation of the cooling rate after sintering is expected to influence the width of microcracks, then the volume fraction of intergranular microcracks and consequently the flexibility of the material. This point is studied in the next section.

#### *Influence of the cooling rate*

Figure 8 shows the effect of the cooling rate on the flexibility of samples sintered at 1600 °C.

One observes that in both cases (8 and 16 h dwell times) a slower cooling induces a higher flexibility. In the same time, the strength of the samples remains relatively equal.

SEM characterization of the microstructure after these four heat treatments showed that for a same grain size (which depends on sintering temperature and dwell time), the microcrack width increases with the cooling time, as reported in Table 3.

Figure 8 clearly shows that a low cooling rate, which promotes crack opening, leads to a higher flexibility.

#### *Study of selected samples*

In order to simplify the comparison between samples, three types of AT samples have been chosen as references among all the prepared samples: NF, F, and VF.

The three materials are dense with an opened porosity always below 5%. The obtained bulk density is about

**Fig. 8** Influence of the cooling rate on mechanical behavior of AT samples sintered at  $T_S = 1600\text{ }^\circ\text{C}$

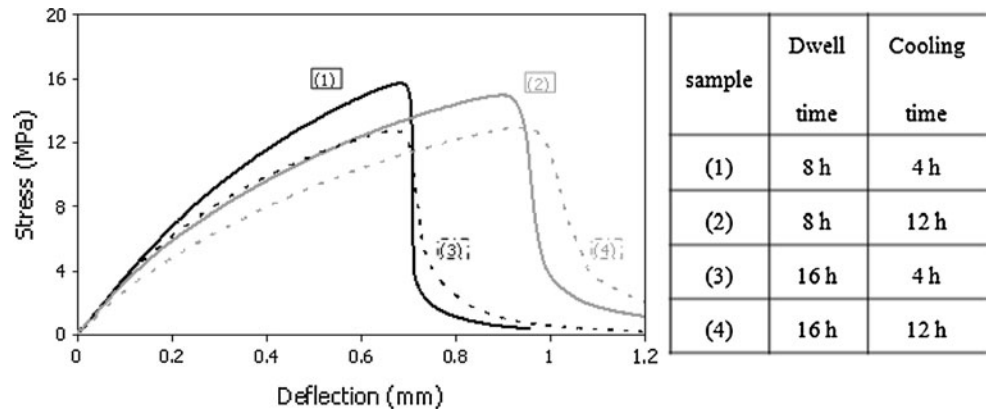


**Table 3** Grain size and microcrack width of samples (1), (2), (3), and (4) evaluated by SEM observations

Sample	(1)	(2)	(3)	(4)
Grain size ( $\mu\text{m}$ )	<150	<150	<200	<200
Microcracks width ( $W_m$ ) (nm)	<150	<300	<250	<500

$3.2\text{ g cm}^{-3}$  for each of them, showing that the densification is identical during their respective sintering cycles: the only differences in their microstructures are grain size and intergranular microcrack array, which lead to different flexibilities.

Table 4 shows their sintering cycle, their microstructure characteristics and their mechanical properties obtained from bending tests (strength and flexibility) and from ultrasonic measurements (Young's modulus).

As its grain size is low, NF sample is just partly microcracked. F sample is sintered at  $1600\text{ }^\circ\text{C}$ , the grain growth is more important and thus grain boundaries are totally microcracked. In VF sample, grain size is even higher due to a longer sintering dwell. The microcracks are wider, allowing to support larger strain in the volume of the sample. One observes also that F and VF have interlocked grains, which help to flexibility.

**Table 4** Sintering cycle, microstructure characteristics, and mechanical properties of the three references of AT samples

/	NF	F	VF
Sintering temperature ( $^\circ\text{C}$ )	1500	1600	1600
Dwell time (h)	1	8	16
Cooling time (h)	4	4	12
Grain size ( $\mu\text{m}$ )	<20	<150	<200
Grain boundary microcracking state	Partly	Totally	Totally
Microcracks width (nm)	<100	<150	<500
Strength (MPa)	18	16	13
Deflection at rupture (mm)	0.27	0.7	1
Young's modulus (GPa)	11.7	7.1	3.6

### Mechanical behavior

The behavior of the materials under three-points bending solicitation is shown in Fig. 9.

The NF sample has brittle behavior featuring a wide linear elastic zone with no post-peak occurrence, as typical ceramic materials. F and VF samples have non linear evolution that leads to a higher flexibility associated to a post-peak behavior which is more marked for the VF sample. These samples seem to have a better adaptability to larger level of strain than NF sample. As previously mentioned, a major parameter for flexibility is the microcrack volume fraction within the sample. The higher this ratio is, the more flexible the material is. Therefore, in order to obtain a high flexibility, the grain boundaries have to be completely microcracked (so that the microcracked grain boundary surface density is equal to the grain boundary surface density) and the average microcrack width has to be substantial. Grain boundaries are only partly microcracked in the case of NF samples and are completely microcracked in the case of F and VF samples. Moreover, VF has wider grain boundary microcracks (up to approximately 500 nm)

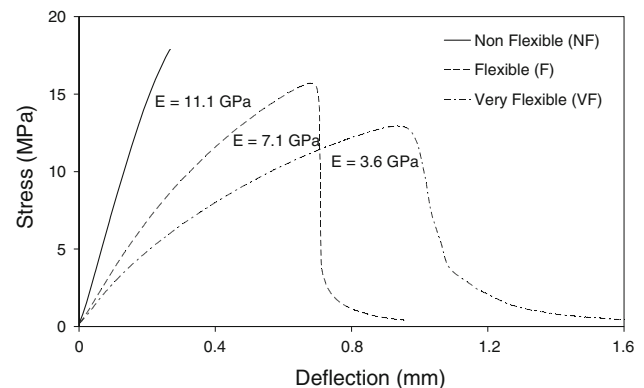


**Fig. 9** Three-points bending test results of the three types of AT samples. Young's moduli have been measured by ultrasonic pulse-echography

than F (up to approximately 150 nm). Consequently, VF presents the highest flexibility.

Of course this flexibility is associated to a decrease in Young’s modulus as classically found for microcracked materials.

*Thermal expansion analysis*

It is well-known that in AT ceramics the large anisotropy in thermal expansion introduces grain boundary cracking during the cooling period from their fabricating temperatures [7]. This grain boundary cracking causes low thermal expansion (or even negative) of the materials and induces a dependence of the thermal expansion on microstructure [11, 12]. Therefore, the different types of AT samples that are considered in this study are expected to have different thermal expansion behaviors.

In a similar way reported in the literature [11], Fig. 10 presents the normalized thermal expansion curves of NF, F, and VF AT samples plotted from 1200 °C during the cooling stage. These curves are helpful in order to estimate the microcracks volume ratio. Indeed, if one assumes that the diffuse damage present in the material exhibits an isotropic propagation, the microcracks volume ratio can be estimated as following:

$$\frac{\Delta V}{V} \Big|_{\mu\text{cracked}} = 3 \times \frac{\Delta L}{L} \Big|_{\mu\text{cracked}} \tag{1}$$

At the beginning of the cooling step, the microcracks are closed, thus the coefficient of thermal expansion (CTE), which can be assumed in this part as the average value calculated from the ones associated to each crystallographic axis, is positive (the sample contracts). The high anisotropy in thermal expansion of AT induces stresses that lead to a

reopening of the microcracks at  $T_c$ . This temperature can be seen on dilatometric curves (Fig. 10) as it corresponds to the minimum value of  $\Delta L/L$  during the cooling stage. Below this temperature, while the temperature decreases down to room temperature, the microcracks gradually become reopened. Therefore, the thermal expansion coefficient is negative (the sample expands). The total expansion of the sample during this microcrack reopening depends on the initial microcrack volume fraction within the material.

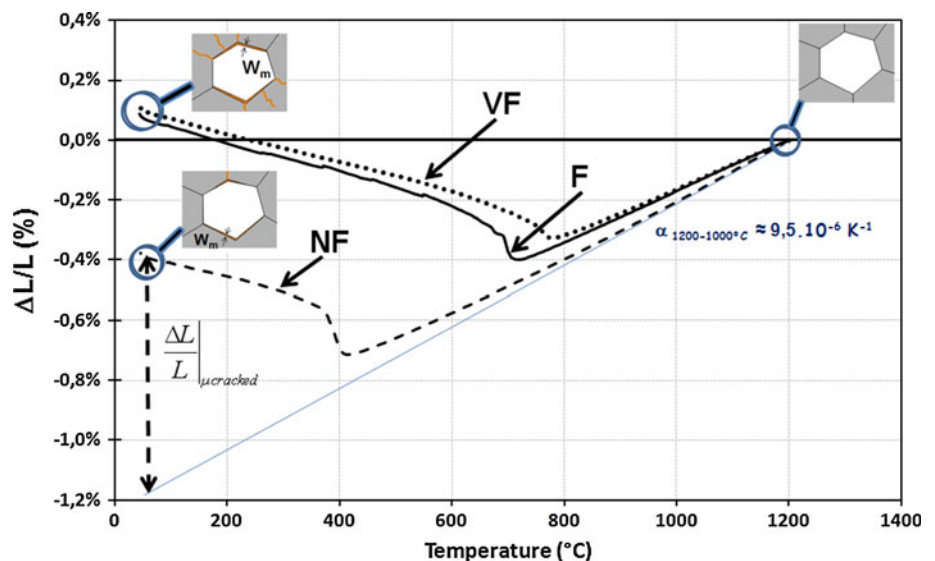
As one can expect, in Fig. 10, the estimated microcracks volume ratio is significantly higher for F and VF samples than for the NF one. This observation is consistent with the global flexible character of each sample.

*Thermal shock resistance*

In the case of AT, thermal shocks can induce stresses in the material by two different manners. The first one, at a macroscopic scale, is the time-dependent thermal gradient within the sample that induces a strain field. The second one, at the scale of the grain, is the characteristic high thermal expansion anisotropy of AT crystal that leads to additional local stresses. The particular microcracked morphology of flexible AT ceramics which leads them to be able to endorse large level strain before rupture is favorable to a good thermal shock resistance. This property depends on the microcrack volume ratio, therefore NF, F, and VF samples are expected to have different thermal shock resistance. Figure 11 displays the effect of thermal shocks on the bending strength of the three types of AT samples as determined by the procedure depicted in section devoted to the “Thermal expansion measurement.”

One can see that NF has a relatively low thermal shock resistance, as the first thermal shock cycle reduces its

**Fig. 10** Thermal expansion behavior of NF, F, and VF samples plotted during the cooling stage from 1200 °C to room temperature



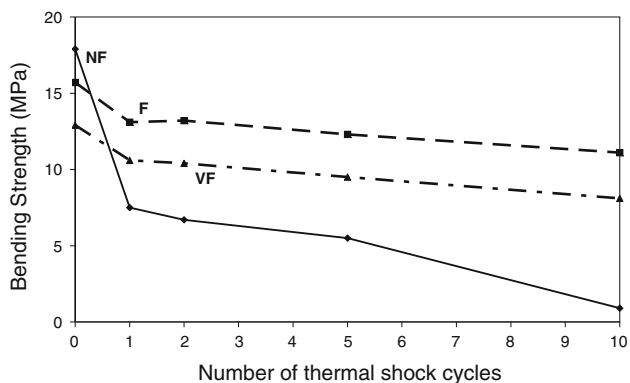


**Fig. 11** Bending strength (MOR) of NF, F, and VF AT samples before and after thermal shock cycles

bending strength by more than 50%. Moreover, additional thermal shocks also induce subsequent damages, since the bending strength obtained after ten cycles is close to zero.

In opposite, F and VF samples exhibit a good thermal shock resistance, as their losses in bending strength are lower, even after a high number of thermal shock cycles. Figure 12 shows SEM micrographies of NF samples before and after ten thermal shock cycles.

One can see that the microstructure is altered by thermal shocks as it contains very wide microcracks (about 2  $\mu\text{m}$ ). This sample is also characterized by much wider cracks that can be observed even at a macroscopic scale. These macrocracks dramatically reduce the strength. The material

is so damaged because its thermal shock resistance is relatively low. In opposite, these ten thermal shock cycles induce no substantial damages in microstructure of VF sample (Fig. 13) as its thermal shock resistance is high.

## Conclusion

Flexible AT ceramics have been elaborated by mimicking itacolumite, a natural flexible sandstone. This material is subjected to a grain boundary microcracking during cooling process after sintering due to its high thermal expansion anisotropy, which can lead to obtain flexible ceramics.

A first study has been carried out, investigating the cause-and-effect link between sintering thermal cycle, microstructure, and mechanical properties (especially flexibility). A substantial amount of AT samples sintered at different sintering cycles has been studied. A clear effect of both sintering temperature and dwell time has been revealed. It turns out that the cooling rate after sintering has also an effect on microstructure and flexibility. Following the results of this work, three types of AT samples have been designed as references: NF, F, and VF. Considering these samples as model refractory materials, their thermal and mechanical behaviors have been more deeply investigated.

A major parameter for flexibility is the microcrack volume fraction within the sample. NF has brittle behavior featuring a wide linear elastic zone, as typical ceramic

**Fig. 12** SEM micrographies of NF AT samples **a** before ten thermal shock cycles, **b** after ten thermal shock cycles

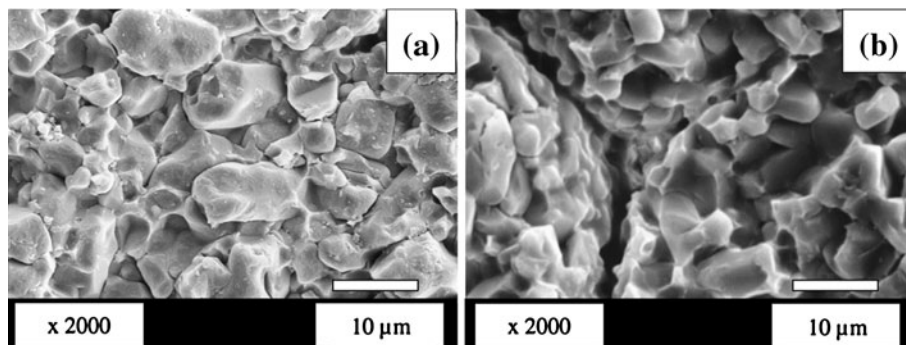
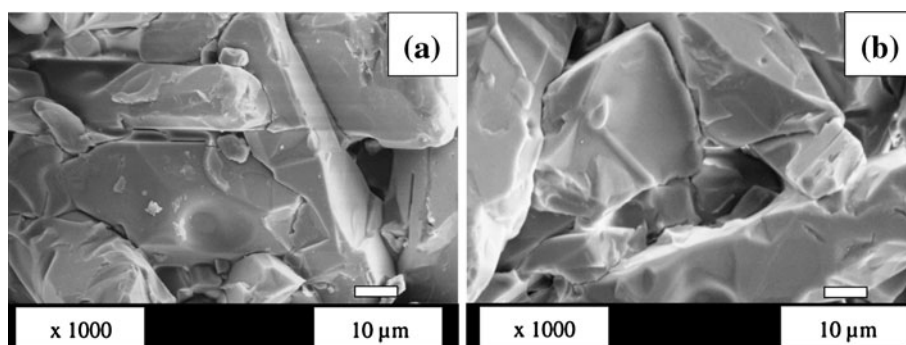


**Fig. 13** SEM micrographies of VF AT samples **a** before ten thermal shock cycles, **b** after ten thermal shock cycles





materials. Conversely, F and VF have nonlinear ductile behavior that leads to a higher flexibility. These samples can resist higher strain. These properties are due to grain boundary microcracks network and to the interlocking of grains. VF is more flexible than F because its microcracks are wider.

Experiments have shown that F and VF samples have a higher thermal shock resistance than NF. This shows that creating flexibility in a ceramic material increases its thermal shock resistance. Flexibility improves the resistance to differential expansion, which is induced by thermal shocks. Furthermore, the microcracks network also enhances the thermal shock resistance. Moreover, thermal shocks slightly raise the average microcrack width, which increases itself the flexibility, thus slightly improving the thermal shock resistance.

The AT ceramics have a very low (or even negative) thermal expansion because of grain boundary microcracks. Thermal expansion measurements have shown that the microcracks become closed during heating (because the individual grains expand into the microcracks) and that a reopening occurs during cooling. This reopening is characterized by an expansion that depends on the initial microcrack volume within the material.

**Acknowledgements** The authors are grateful to the Federation for International Refractories Research and Education (FIRE) for its financial support.

## References

1. Hasselman DPH (1969) *J Am Ceram Soc* 11:3600
2. Aksel C, Warren P (2003) *J Eur Ceram Soc* 23:301
3. Hugot F, Glandus JC (2007) *J Eur Ceram Soc* 27:1919
4. Andreev K, Harmuth H (2003) *J Mater Process Technol* 143–144:72
5. Doncieux A, Stagnol D, Huger M, Chotard T, Gault C, Ota T, Hashimoto S (2008) *J Mater Sci* 43:4167. doi:[10.1007/s10853-007-2414-z](https://doi.org/10.1007/s10853-007-2414-z)
6. Sato I, Ichikawa Y, Sakanoue J, Mizutani M, Adachi N, Ota T (2008) *J Am Ceram Soc* 91:607
7. Bayer G (1971) *J Less-Common Met* 24:129
8. Bhardwaj M (1986) *Adv Ceram Mater* 1:311
9. Kulkarni N, Moudgil B, Bhardwaj M (1994) *Am Ceram Soc Bull* 73:146
10. Kim HC, Lee KS, Kweon OS, Aneziris C, Kima IJ (2007) *J Eur Ceram Soc* 27:1431
11. Ohya Y, Nakagawa Z (1996) *J Mater Sci* 31:1555. doi:[10.1007/BF00357864](https://doi.org/10.1007/BF00357864)
12. Hasselman DPH, Donald KY (1996) *J Eur Ceram Soc* 76:2180